Investigations Into Nonuniform Photonic-Bandgap Microstripline Low-Pass Filters

Nemai Chandra Karmakar, *Senior Member, IEEE*, and Mohammad Nurunnabi Mollah

***Abstract*—With the advent of planar photonic bandgap (PBG) materials, different PBG topologies have been proposed to improve bandgap performances of microwave signals. Conventional circular-patterned PBGs have constraints in the wide stopband performance due to high passband ripples. In this paper, we suggest two novel configurations with nonuniform dimensions of circular-patterned PBGs to improve the stop bandwidth and passband ripples. The dimensions of PBG units are varied proportionally to the coefficients of *binomial* and *Chebyshev* polynomials. The simulated and measured responses of the proposed PBG units are presented. It is seen that Chebyshev distribution produces excellent performance by suppressing passband ripples and producing distinct stopband. These performances of passband ripples and stop bandwidth are further improved with Chebyshev distributed annular-ring PBG units with their unique feature of aspect ratio control.**

***Index Terms*—Annular-ring photonic bandgap (PBG), binomial and Chebyshev distributions, filters, microstrip lines, passband, photonic bandgap (PBG), ripples, stopband.**

I. Introduction

PLANAR photonic bandgap (PBG) structures are a class of periodic dielectrics, which are the photonic analogs of semiconductors. Electromagnetic waves behave in photonic substrates as electrons behave in semiconductors. PBGs exhibit wide bandpass and band-rejection properties at microwave and millimeter-wave frequencies and have offered tremendous applications in active and passive devices [1]–[3]. Introducing periodic perturbation such as dielectric rods, holes, and patterns in waveguides and microstrip substrates forms PBG materials. While various configurations have been proposed in literature, only the planar etched PBG configurations [1]–[12] have attracted much interest due to their ease of fabrication and integration with other circuits with photolithographic processes.

The behavior of PBG-engineered materials can be controlled with the proper choice of different lattice structures and lattice parameters such as the filling factor, patterns/geometries of perturbations, and distributions of PBG units. Lopeteg *et al.* [7] report sinusoidal and triangular patterns along with the conventional circular pattern. Laso *et al.* [6] report a nonuniform distribution and tapering the radii of circular PBG patterns with Gaussian distribution and chirped periods. Yun and Chang [12] report uniplanar one-dimensional (1-D) PBG structures and resonators on coplanar waveguides, slot lines, and coplanar striplines. Different resonator lines with PBG reflectors are used to investigate the stopband filter characteristics. The reported configurations have produced different results on the improvement of the stopband performance and suppression of ripples near cutoff frequencies over the conventional hole (circular pattern) PBG units.

In this paper, we propose novel PBG structures in the form of nonuniform distributions of circular and annular-ring patterns to investigate any improvement over the conventional uniform circular-patterned PBG. Two distributions—*binomial* [9] and *Chebyshev* [10] polynomials—as applied to antenna array synthesis, are used to taper the dimensions of the etched circular and annular-ring-patterned PBG units on the ground plane of a standard microstrip transmission line. While the uniform distribution of the circular-patterned PBG [4] is hindered with high passband ripples near the cutoff frequency, the nonuniform distributions in the forms of binomial and Chebyshev polynomials yield superior performances by suppressing passband ripples and producing distinct wide stopband. The novelty of the proposition is that binomial and Chebyshev polynomials are exploited to control the low-pass filter (LPF) response and selectivity. Hence, the filter synthesis is substantially relaxed in the present approach. The depth of passband return loss (RL), selectivity, and the ripples can also be controlled with the sidelobe level (SLL) index of a Chebyshev polynomial. Since the passband ripple height increases with the filling factor, the uniform circular-patterned PBG limits the wide-band applications. Using the nonuniform distribution of PBG patterns, both passband ripple and stop bandwidth problems are alleviated and the selectivity of the stopband of planar PBGs increases. The novel finding can be very useful for wide-band surface-wave suppression [5]–[12] in planar and microstrip antennas, diplexers, filters, and amplifiers.

The following sections present the theory of binomial and Chebyshev polynomials as applied to low-sidelobe array theory and tapered impedance-matching sections. The selectivity of the LPF is defined. The design procedure of uniform and nonuniform circular- and annular-patterned PBG units is presented below. Results of ten-element circular- and annular-patterned PBG arrays in uniform, binomial, and Chebyshev distributions are presented and compared and are followed by conclusions.

Manuscript received June 15, 2002. This work was supported under the Agency for Science, Technology, and Research (A*STAR) Strategic Research Program on Micro-electromechanical Systems for Automatic Identification and Tracking (MEMSAIT) Project NSTB/43/11/4–3.

The authors are with the Global Positioning System Center, School of Electrical and Electronic Engineering, Nanyang Technological University, Singapore 639798 (e-mail: Enckarma@ntu.edu.sg).

Digital Object Identifier 10.1109/TMTT.2002.807817

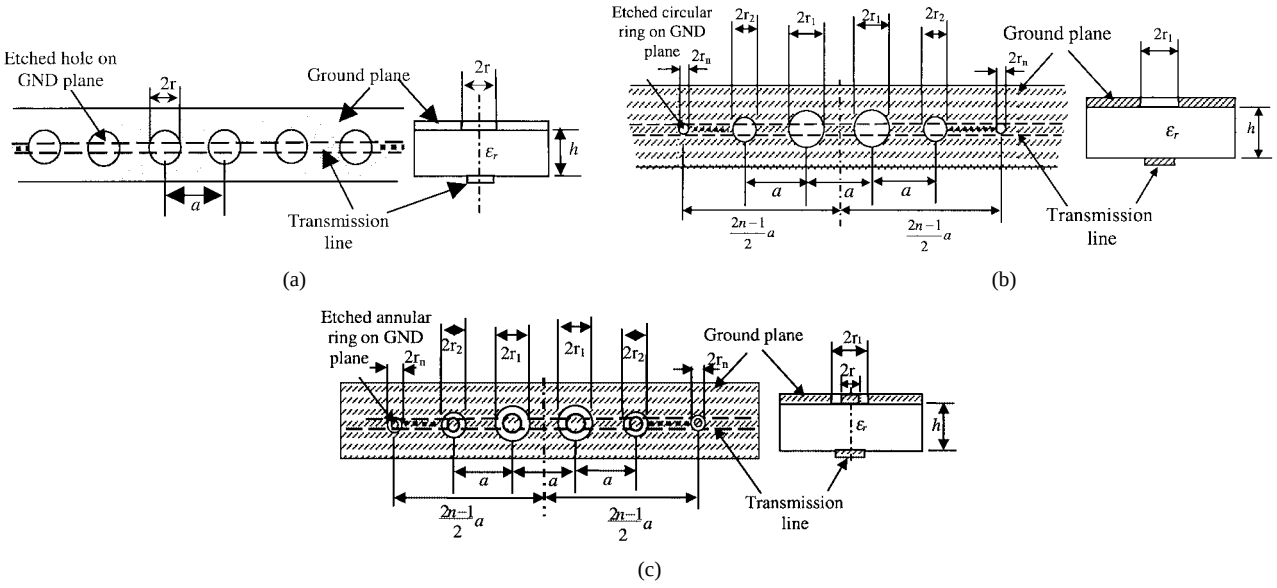

Fig. 1. (a) Uniform circular-patterned PBG with period "a" and radius "r." (b) Nonuniform circular and (c) nonuniform annular ring patterned of even-numbered PBG units.

II. Theory of Nonuniform 1-D Microstrip PBGs

A. Binomial Distribution

A maximally flat passband transmission characteristic is obtained when the coefficient of the polynomial [13], [14] is determined by the following expression:

$$(1+x)^{m-1} = 1 + (m-1)\,x + \frac{(m-1)\,(m-2)}{2!}x^2 + \frac{(m-1)\,(m-2)\,(m-3)}{3!}x^3 + \cdots. \quad (1)$$

The positive coefficients of the series expansion for different values of m are expressed in terms of Pascal's triangle [13]. If the values of m represent the number of elements in an array, the coefficients of the expansion represent the relative amplitudes of the elements. Generally, this type of array suffers from practical limitation of bandwidth and efficiency due to the abrupt change in amplitude tapering between adjacent elements. In this study, we vary the dimensions of circular PBGs proportionally to the relative amplitudes of the polynomial.

B. Chebyshev Polynomial

Instead of maximally flat passband characteristics, an equally useful characteristic is one that may permit the transmission coefficient to vary with minute ripples over the stopband [13]. This provides a considerable increase in bandwidth with respect to binomial distribution. This equal-ripple characteristic is obtained by making the distribution according to the Chebyshev polynomial. The basic properties of the polynomial [13] are expressed as follows:

$$T_m(z) = 2zT_{m-1}(z) - T_{m-2}(z) \quad (2)$$

where $T_m(z)$ is expressed as

$$T_m(z) = \cos\left[m\cos^{-1}(z)\right] \text{ for } |z| \le 1. \quad (3)$$

The coefficients of the polynomial are determined for any prescribed SLL. In the design example, we take a ten-element PBG array with a tapered distribution according to Chebyshev coefficients. For a prescribed voltage ratio between the peak and SLL, e.g., for 25 dB, the amplitudes are determined as follows:

$$0.36 \quad 0.49 \quad 0.71 \quad 0.78 \quad 1 \quad 1 \quad 0.78 \quad 0.71 \quad 0.49 \quad 0.36.$$

Amplitude 1 is for the two center elements of the ten-element array and the rest of the elements follow suit. For our PBG design, we shall vary the radii and areas of the circles and annular rings proportionally to the relative amplitudes, respectively.

C. Selectivity of LPFs

One important parameter of the filter is the selectivity at 3-dB cutoff frequencies. We define the selectivity of the LPF as

$$\xi = \frac{\alpha_{\min} - \alpha_{\max}}{f_s - f_p}\left(\frac{\text{dB}}{\text{GHz}}\right) \quad (4)$$

where ξ = selectivity in decibels/gigahertz, $\alpha_{\max}$ = the 3-dB attenuation point, $\alpha_{\min}$ = 20-dB attenuation point, f_s = 20-dB stopband frequency in gigahertz, and f_p = 3-dB cutoff frequency in gigahertz.

In this paper, we shall show how the selectivity of the PBG-engineered LPF will improve with binomial and Chebyshev distributions.

III. Design of 1-D Microstrip PBGs

Fig. 1 shows three different varieties—*uniform* circular and *nonuniform* circular and annular-ring-patterned planar PBGs on microstrip substrates. As can be seen in this figure, the uniform [cf. Fig. 1(a)] and the nonuniform circular [cf. Fig. 1(b)] patterns are etched with a period "a" on the ground plane of standard microstrip transmission lines to form a PBG-engineered microstrip transmission line. The important design parameters to achieve a stopband characteristic are the period "a" and the filling factor "r/a." For the uniform circular-patterned PBG, the

circles are of same radius "r" and period "a." For nonuniform patterned PBGs, the center elements have the largest radii of "r_1," which are proportional to coefficient 1, and the radii of the adjacent circles decrease proportionally to the amplitude coefficients of the polynomials. For Chebyshev distribution, the area of the PBG patterns will vary proportionally to the coefficients of the polynomial for a particular SLL (voltage ratio). Here, we propose two distinct relationships between amplitudes of the coefficients of the polynomials and the physical dimensions of the PBG circles. They are: 1) polynomial coefficient's amplitudes are proportional to the radius of the PBG circle (r), called type 1, and 2) polynomial coefficient's amplitudes are proportional to the areas of the PBG circles (πr^2), called type 2. The tapering of the physical dimensions of the PBGs for both types 1 and 2 follows the coefficients of the polynomial taking the central elements as reference. The period and filling factor (r/a) of the PBG line determine the dimensions (radii) of the central elements. The investigations are carried out with the two types of PBG configurations with circular patterns and the respective results are shown in Section IV.

The center frequency of the stopband is calculated approximately with the following expression:

$$\beta a = \pi \tag{5}$$

where a = the period of the PBG pattern and β = the wavenumber in the dielectric slab. β is defined by (6) as follows:

$$\beta = \frac{2\pi f_0}{c}\sqrt{\varepsilon_e} \tag{6}$$

where f_0 = the center frequency of the stopband, ε_e = the effective relative permittivity of the dielectric slab, and c = the speed of light in free space. Using (5) and (6), the period for any stopband frequency can be determined. For an N-element PBG patterns, the nth element's location from the center of the PBG period can be derived from the following equation:

$$d_n = \begin{cases} \dfrac{2n-1}{2}a, & \text{for even } N \\ (n-1)a, & \text{for odd } N. \end{cases} \tag{7}$$

Fig. 1(b) and (c) shows such distributions for even N.

IV. Results

In our study, we use RT/Duroid 6010 with $\varepsilon_r = 10.2$ and thickness $h = 25$ mil. The center frequency is selected at 10 GHz and the period $a = 224$ mil. Based on the design parameters, two different distributions—the binomial and Chebyshev distributions of PBG patterns—have been designed and analyzed. The PBG structures are simulated with the method-of-moments (MOM)-based software tool Zeland IE3D. The following sections present the results of dispersion characteristics in terms of S-parameters versus frequency for: 1) uniform; 2) binomial; and 3) Chebyshev distributions. Due to the unrealizable dimensions of the last few PBG units of binomial distribution, we confine the study of binomial distribution PBG units into theoretical investigations only.

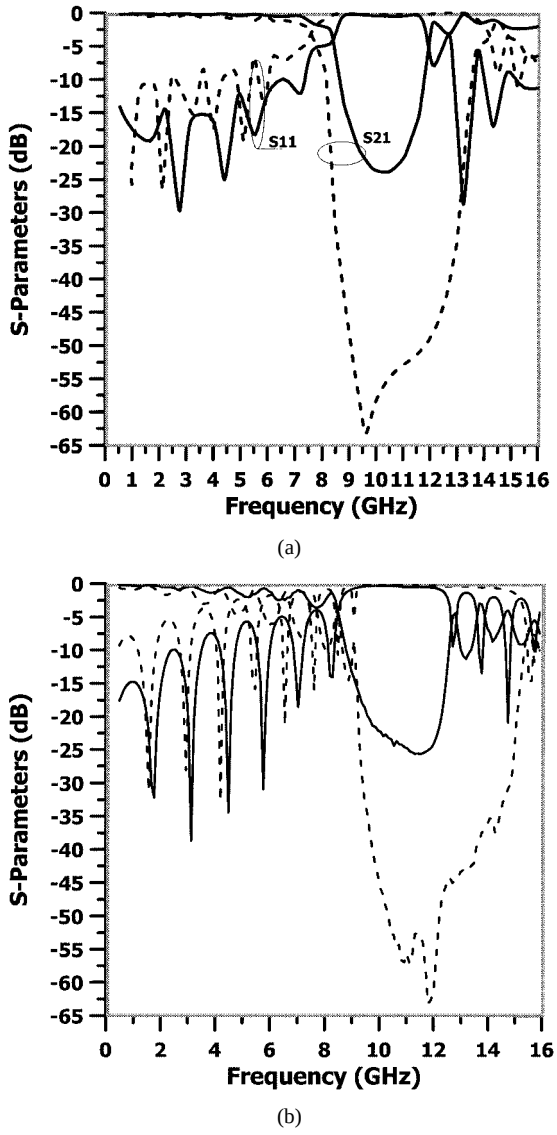

Fig. 2. S-parameter versus frequency for different radii of the uniform circular PBG lines. (a) Simulated and (b) measured results. Solid lines: $r = 56$ mil, dotted lines: $r = 84$ mil with a period $a = 224$ mil, linewidth 24 mil (50 Ω). Dielectric substrate: $\varepsilon_r = 10.2$, $h = 25$ mil.

A. Uniform 1-D Microstrip PBG

Fig. 2 shows the S-parameters versus frequency for two different filling factors $r/a = 0.25$ ($r = 56$ mil) and $r/a = 0.375$ ($r = 84$ mil) for the uniform distribution of circular patterns with a period of 224 mil. As can be seen in this figure, the filling factor plays important role in determining the rejection bandwidth. For $r = 56$ mil (solid lines), the 20-dB (S_{21}) rejection bandwidth is 1.89 GHz, while for $r = 84$ mil (dotted lines), the 20-dB rejection bandwidth is 4.95 GHz. As shown in Fig. 2(b), the ripples in S-parameters near the cutoff frequencies and in the low-pass region are significantly high and no distinct low-pass response is observed for both cases. As can be seen, near (3-dB S_{21}) cutoff frequencies, the RL is less than 5 dB for $r = 56$ mil and close to 0 dB for $r = 84$ mil. Over the low-pass region, both the RL and insertion-loss performances are very poor for both cases. It is also worthwhile to note that, with the filling factor, the center frequency of the rejection band increases slightly.

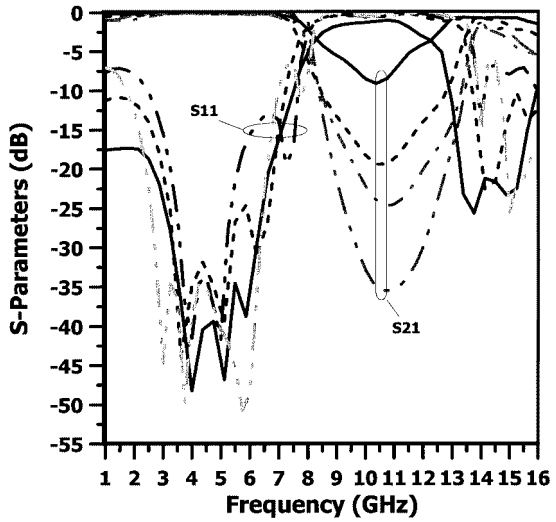

Fig. 3. S-parameter versus frequency for different radii of the circular PBG lines with binomial tapering. Type 1—solid lines: $r_1 = 56$ mil, dotted lines: $r_1 = 84$ mil, dotted–dashed lines: $r_1 = 110$ mil; type 2—double dotted–dashed line: $r_1 = 110$ mil with a period $a = 224$ mil, linewidth 24 mil (50 Ω). Dielectric substrate: $\varepsilon_r = 10.2$, $h = 25$ mil.

Comparing the measured and simulated results it can be concluded that the measured low-pass ripples are significantly high. Therefore, it is not an LPF at all. The measured frequency shifts a little in the higher frequency region and the stop bandwidth is larger than that for the simulated results. The discrepancies can be attributed to the dielectric and conductor loss in the microstrip lines, and fabrication tolerances and errors, which are not considered in the simulation. In general, the agreement is quite good.

To improve the performance of the conventional circular-patterned PBGs, two nonuniform distributions—binomial and Chebyshev polynomial distributions—for circular-patterned PBGs are proposed. Followings are the results to show how the S-parameter performances have improved.

B. Binomial Distribution of Circular-Patterned PBG

Fig. 3 shows the simulated S-parameters versus frequency with the filling factor as a parameter for the binomial distribution of a circular-patterned PBG with a period of 224 mil. The radii of the largest circles are 56 mil (solid lines), 84 mil (dashed lines), 110 mil (dotted–dashed line) for type 1 (where the radii of the circles are proportional to the polynomial coefficients), and 110 mil (double dotted–dashed line) for type 2 (where the areas of the circles are proportional to the polynomial coefficients). As can be seen in this figure, the filling factor plays an important role in determining the rejection bandwidth. Consequently, the ripples at the cutoff frequencies and the low-pass frequencies have improved considerably. The center frequency of the rejection band has shifted slightly upward with the radius (filling factor r/a). Table I summarizes the results. As can be seen, $S_{21(\max)}$ in the rejection band increases with the filling factor and the 20-dB isolation bandwidth also increases. The last two shaded rows show the comparison between the two types of distributions. As can be seen in Table I, the rejection bandwidth and selectivity have increased considerably in type 2 compared

TABLE I
COMPARATIVE STUDY OF CIRCULAR PATTERNED PBGs WITH BINOMIAL DISTRIBUTION: $\varepsilon_r = 10.2$, $h = 25$ mil, PERIOD $a = 224$ mil

Type	r_1 (mil)	Stopband Isolation		1st null RL (dB)	20dB Isolation BW (GHz)	Selectivity: dB/($f_2 - f_0$) (dB/GHz)	20dB Pass-band RL BW (GHz)
		$S_{21\max}$ (dB)	f_0 (GHz)				
Type 1: x ∝ r	56	8	10.2	38	0	0	4.125
	84	20	10.4	32	0	5.66	3.875
	110	25	10.6	20	2.5	11.33	2.375
Type: 2 x ∝ area	110	35	10.6	11	4	21.25	4.25

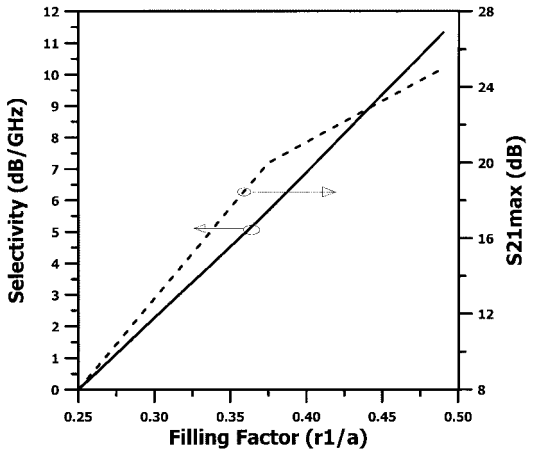

Fig. 4. Selectivity and maximum isolation versus filling factor for the circular-patterned PBGs with the binomial distribution with a period $a = 224$ mil, linewidth 24 mil (50 Ω). Dielectric substrate: $\varepsilon_r = 10.2$, $h = 25$ mil.

to type 1. Also in the low-pass region, the 20-dB RL bandwidth has improved.

1) Selectivity : As can be seen in Fig. 4, the selectivity of the LPF, as well as the depth of the transfer function ($S_{21\max}$) in the rejection band increase with the filling factor. With a filling factor of 0.25, the selectivity was zero and, at a 0.49 filling factor, the selectivity has increased to 21.25 dB/GHz. $S_{21\max}$ in the rejection band also increases from 8 dB for a filling factor of 0.25 to 25 dB for a filling factor of 0.49.

2) Passband RL Characteristics: Fig. 5 shows the low-pass characteristics of the binomially distributed PBG circles. The 20-dB passband RL bandwidth and the first null of RL near the cutoff frequency increase with the filling factor. This means that, while the filling factor for conventional uniform circular-patterned PBGs generates ripples, the problem can be alleviated significantly with the binomial distribution of the PBG patterns.

3) Tandem of Two Binomially Distributed PBG Lines: Finally, two ten-element circular PBGs are connected in tandem. The total length of the line is double than that for a single ten-element circular PBG line. Fig. 6 shows the S-parameters versus frequency for the tandem binomially distributed (type 1) 20-element circular PBG line. The filling factor of 0.375 ($r = 84$ mil) with the period of 224 mil is used. Comparing Figs. 3 and 5, it can be concluded that the tandem PBG line has improved the stopband and low-pass

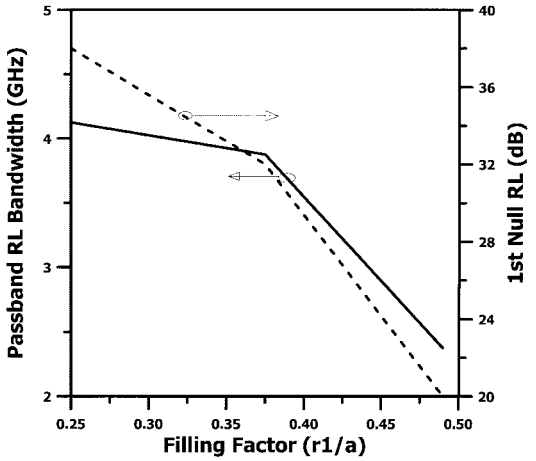

Fig. 5. Lower passband RL bandwidth and first null RL versus filling factor for the circular-patterned PBG with binomial distributions with a period $a = 224$ mil, linewidth 24 mil (50 Ω). Dielectric substrate: $\varepsilon_r = 10.2$, $h = 25$ mil.

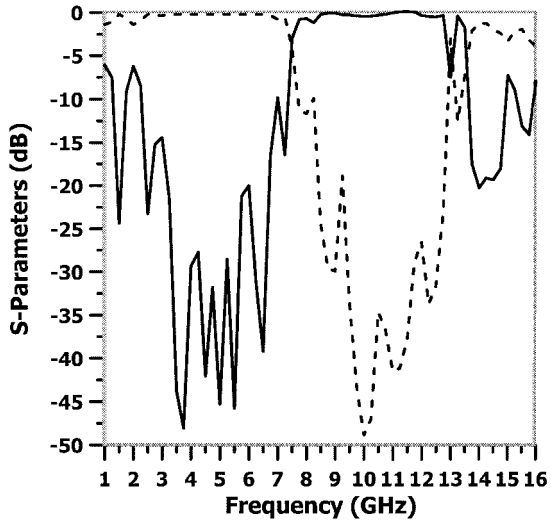

Fig. 6. S-parameter versus frequency for a cascade of two ten-element circular-patterned PBG lines with binomial distribution (type 1) with $r_1 = 56$ mil, a period $a = 224$ mil, and linewidth 24 mil (50 Ω). Dielectric substrate: $\varepsilon_r = 10.2$, $h = 25$ mil.

performances significantly. While the ten-element binomial line has no stopband, in the 20-element tandem line, the stopband bandwidth is 4.86 GHz and 20-dB passband RL bandwidth is 3.87 GHz. Therefore, by cascading two binomially distributed lines, we can improve the stopband and passband performances of the PBG structures.

Once we have investigated the characteristics of binomially distributed circular PBGs, we next present the performances for Chebyshev distributions of circular PBGs.

C. Chebyshev Distribution

While binomial distribution suffers from narrow-band performance and poorer low-pass selectivity, the performance can be improved significantly with the Chebyshev distribution. Fig. 7 shows the measured and simulated S-parameters. As can be seen, the measured passband ripples have reduced significantly similar to that for an ideal transmission line, whereas in uniform distribution, the ripples were very high in the passband region.

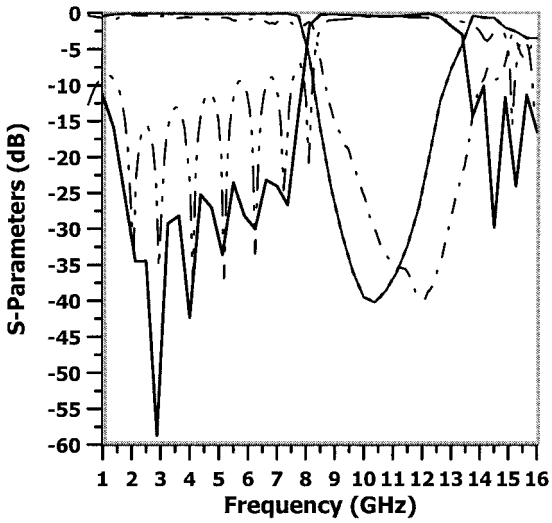

Fig. 7. S-parameter versus frequency for a ten-element circular-patterned PBG line (type 1) with 25-dB SLL Chebyshev polynomial distribution with $r_1 = 84$ mil, a period $a = 224$ mil, and linewidth 24 mil (50 Ω). Dielectric substrate: $\varepsilon_r = 10.2$, $h = 25$ mil. Solid line—simulated and double dashed–dotted lines—measured results for -25-dB SLL.

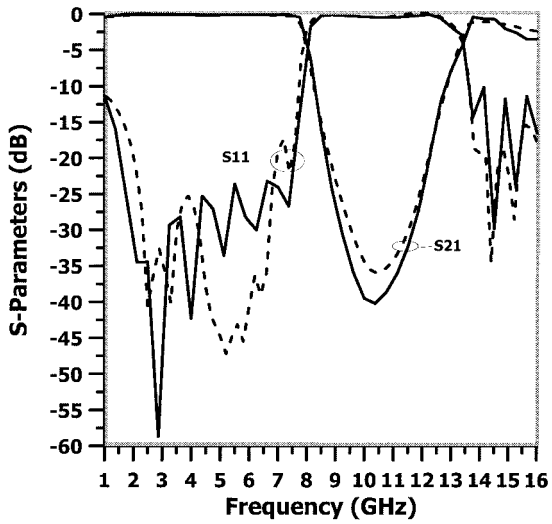

Fig. 8. S-parameter versus frequency for a ten-element circular-patterned PBG line with 25-dB SLL Chebyshev polynomial distribution (type 1) with $r_1 = 84$ mil, a period $a = 224$ mil, and linewidth 24 mil (50 Ω). Dielectric substrate: $\varepsilon_r = 10.2$, $h = 25$ mil. Solid line -25 dB; dotted line -35 dB.

This is a significant improvement over the uniform circular-patterned PBG transmission lines, as shown in Fig. 2. However, in this case, the stop bandwidth has reduced with respect to the uniform circular-patterned PBG with $r = 84$ mil. As usual, we see there is a measured stopband resonant frequency shift due to the fabrication errors of the PBG-engineered line. Comparing the measured results alone in Figs. 2 and 7, it can be concluded that the improvement of the Chebyshev distributed circular-patterned PBG is very significant as an LPF design where filter synthesis has been greatly reduced due to the implementation of a simple Chebyshev polynomial.

1) Prescribed SLL (25 and 35 dB): Fig. 8 shows the S-parameters versus frequency response for a ten-element circular-patterned PBG line (type 1) with Chebyshev polynomial distributions with two prescribed SLLs of 25 dB (solid line)

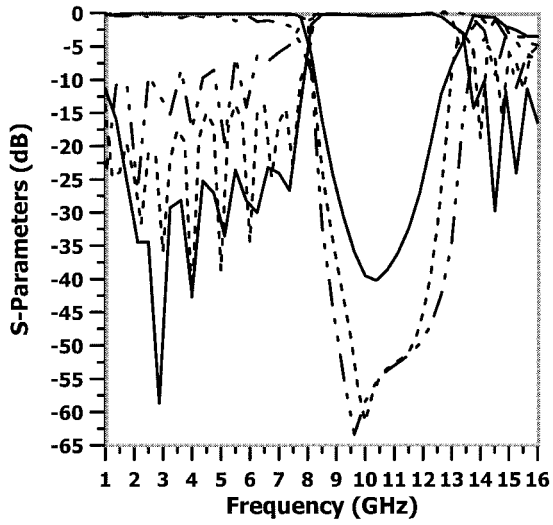

Fig. 9. S-parameters versus frequency for a ten-element circular-patterned PBG line with 25-dB SLL Chebyshev distribution with $r_1 = 84$ mil, a period $a = 224$ mil, and linewidth 24 mil (50 Ω). Dielectric substrate: $\varepsilon_r = 10.2$, $h = 25$ mil. Solid line—Chebyshev (type 1); dotted line—Chebyshev (type 2), double dotted–dashed line—uniform distribution.

TABLE II
COMPARATIVE STUDY OF CIRCULAR PATTERNED PBGS WITH UNIFORM AND CHEBYSHEV DISTRIBUTIONS: $\varepsilon_r = 10.2$, $h = 25$ mil, $r = 84$ mil, PERIOD $a = 224$ mil

Type	Stopband Isolation		20 dB Isolation BW (GHz)	Selectivity: dB/($f_s - f_p$) (Lower cutoff) (dB/GHz)	1st null and peak RL (dB)	
	$S_{21(max)}$ (dB)	f_0 (GHz)			Null	Peak
Uniform	63.4	9.6	5.68	21.7	7.2	6.14
Type 1	61.5	10	5.04	20.92	27	24
Type 2	40.3	10.2	4	56.6	23	15

and 35 dB (dotted lines), respectively. As can be seen in this figure, both distributions yield very sharp cutoff performance and the low-pass RL performance has improved significantly. For both cases, the rejection bandwidth is 4.5 GHz, the first null in RL near cutoff is 27 dB and the selectivity is 27 dB/GHz. The two performances are very similar, except the depth in $S_{21\max}$ and first RL nulls. For 35-dB distribution, the first RL null is 17 dB and $S_{21\max}$ is 36 dB.

2) Comparison With Uniform Distribution: Fig. 9 shows the comparison of S-parameter performances with a frequency for uniform and Chebyshev type 1 and 2 distributions for 25-dB SLL voltage ratio. The radii are $r = r_1 = 84$ mil. The results are summarized in Table II. From this figure and table, it can be concluded that Chebyshev type 2 distribution yields similar bandwidth performance to that for the uniform distribution, but the selectivity (20.92 dB/GHz) of type 1 is poorer than that for type 2 (56.6 dB/GHz). For type 2, the selectivity of the filter is much more improved than that for the uniform distribution (21.7 dB/GHz). The characteristic of the filter response near the cutoff also improves significantly for both Chebyshev types. The first null of RL is 27 dB for type 1 and 23 dB for type 2 compared to 7.2 dB for uniform distribution of circular PBGs.

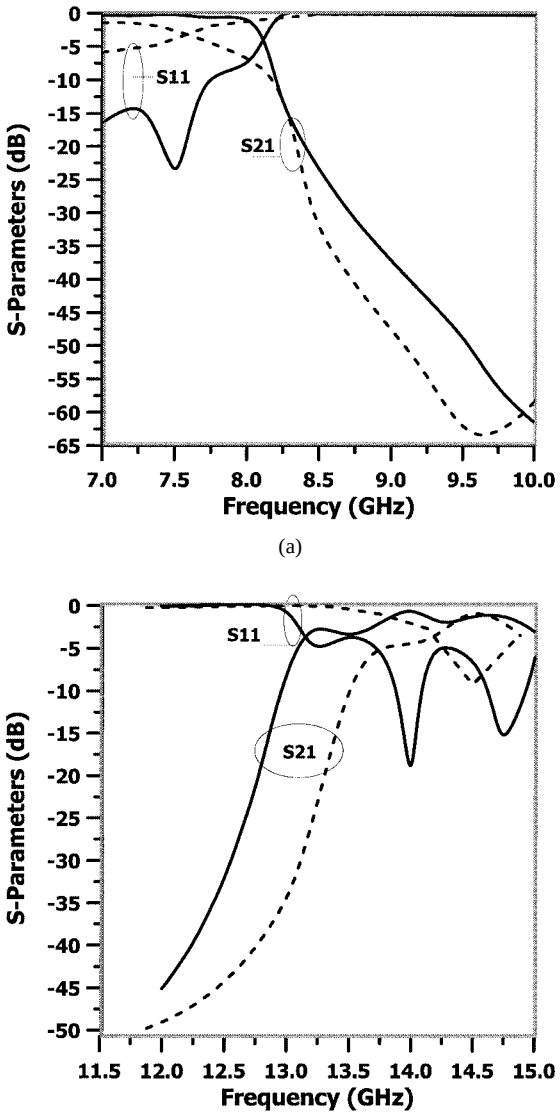

Fig. 10. Analysis of S-parameters at cutoff frequencies for uniform and Chebyshev distribution of ten-element circular-patterned PBG lines. (a) Lower cutoff region. (b) Upper cutoff region. $r_1 = 84$ mil, a period $a = 224$ mil, and linewidth 24 mil (50 Ω). Dielectric substrate: $\varepsilon_r = 10.2$, $h = 25$ mil. Solid line—Chebyshev (type 2); dotted line—uniform.

3) Analysis of Cutoff Performances: Fig. 10 shows the close-up view of the cutoff performances of the S-parameters for uniform and Chebyshev type 2 distribution for $r = r_1 = 84$ mil. As can be seen from Fig. 10(a), the chart for S-parameters near the lower cutoff region, the selectivity for the uniform distribution is 21.7 dB/GHz, while for the Chebyshev type 2 distribution, the selectivity is 56.6 dB/GHz. Fig. 10(b) shows the similar performance at the upper cutoff region where the selectivity is 18.06 and 43.35 dB/GHz for uniform and Chebyshev type 2 distributions, respectively. In both the lower and upper cutoff (3 dB) regions, the RL for the uniform distribution is merely 3 dB, while for Chebyshev type 2 distribution, the RL shows distinct nulls of approximately 20 dB.

4) Filling Factor Near $r_1/a \approx 0.5$: Finally, the performance of the Chebyshev type 1 (dotted lines) and type 2 (solid

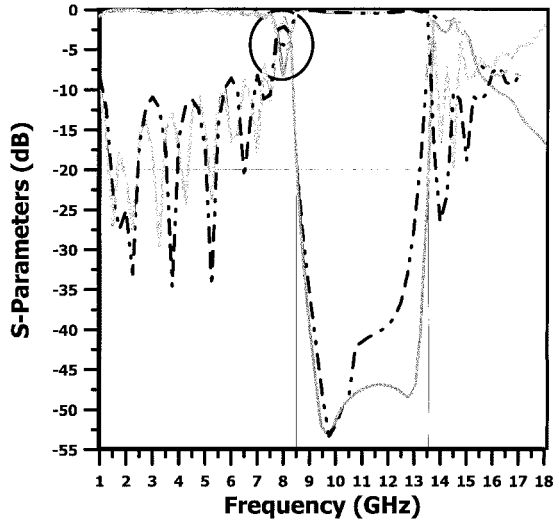

(a)

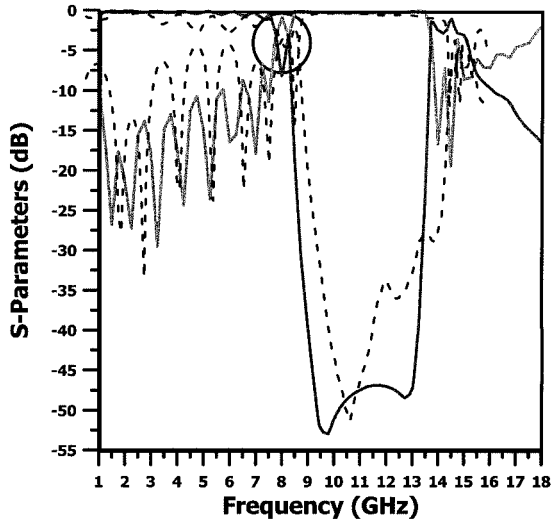

(b)

Fig. 11. (a) Simulated and (b) comparison of measured and simulated results (type 2) S-parameter versus frequency for a larger filling factor ($r/a = 0.49$) for a ten-element circular-patterned PBG line with a 25-dB SLL Chebyshev distribution with $r_1 = 84$ mil, a period $a = 224$ mil, and linewidth 24 mil (50 Ω). Dielectric substrate: $\varepsilon_r = 10.2, h = 25$ mil. Solid line—type 2; dotted line—type 1.

lines) distributed circular-patterned PBGs are investigated near the filling factor of $r_1/a \approx 0.5$, when the two largest circles almost touch each other. Here, $r_1 = 110$ mil for a period of 224 mil has been selected and analyzed for a 25-dB SLL. As can be seen in Fig. 11, for type 2, the rejection band S_{21} is more distinct and larger in bandwidth than that for type 1. The bandwidth is greater than 5 GHz. There are ripples observed for the nonuniform circular PBG (shown here with a circle on the curves), but the passband RL performance is superior to that for the uniform distribution.

Fig. 11(b) shows the measured results for type 2. The results agree very well, except for high passband ripples and wider stop bandwidth. Although the measured passband ripples are much larger than those for the simulated ones, the scenario is much better than those for the uniform circular-patterned PBGs shown in Fig. 2.

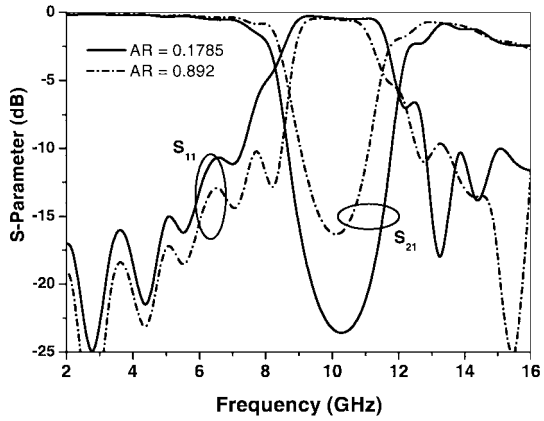

(a)

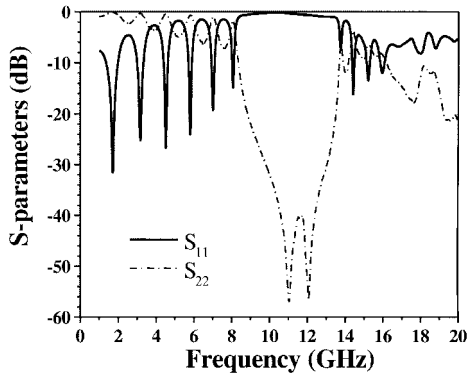

(b)

Fig. 12. (a) Simulated S-parameters versus frequency for annular-ring PBG with different aspect ratios. $R_{\text{out}} = 56$ mil, period 224 mil, substrate: $\varepsilon_r = 10.2, h = 25$ mil. (b) Measured S-parameters versus frequency of aspect ratio $= 0.15$.

D. Annular-Ring-Patterned PBG

In this section, the performance of uniform [15] and nonuniform annular-ring PBG assisted microstrip lines have been demonstrated. Ring PBG structures yield the facilities of aspect ratios. The annular-ring PBGs are studied with respect to their aspect ratio, rejection bandwidth, and passband ripple heights. For the aspect ratio study, the same filling factor, which is the ratio of the outer radius r_1 and period a of the annular ring, is used. The inner ring radius (aspect ratio) is varied and the S-parameter performance is recorded. Microwave material: RT/Duroid 6010 with $\varepsilon_r = 10.2$ and thickness $h = 25$ mil is used in the investigation. The period $a = 224$ mil is used in all investigations. Different uniform and nonuniform annular-ring PBG structures are designed and simulated with the MOM-based software tool Zealand IE3D, and the measured results are compared with the simulated ones.

1) Uniform 1-D Ring PBG: In the annular-ring PBG, the outer dimension has been kept constant, while the inner dimensions have been changed to vary the aspect ratio of the ring PBG unit. Simulation results for aspect ratios $= 0.1785$ and 0.892 are shown in Fig. 12(a). From the simulation results, it is seen that the rejection bandwidth reduces with the aspect ratio. The uniform-ring PBG assisted transmission line yields ripple in the passband. This ripple can be suppressed with nonuniform dis-

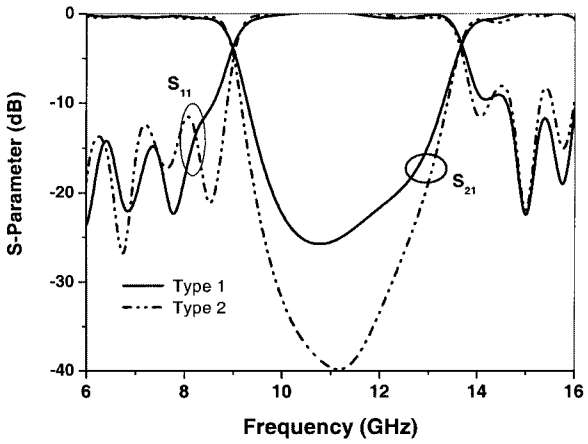

Fig. 13. Simulated result of a 50-Ω transmission line having $w = 24$ mil on a Chebyshev annular-ring-patterned PBG ground plane. Aspect ratio $= 0.15$ (for both type 1 and type 2), $a = 224$ mil, $r_1 = 62.5$ mil, substrate: $\varepsilon_r = 10.2$, $h = 25$ mil.

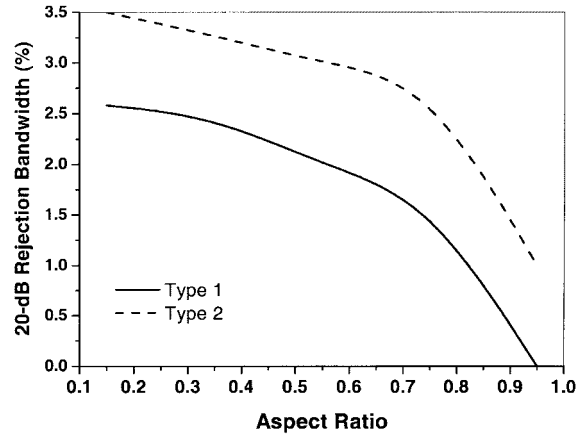

Fig. 14. Variation of bandwidth versus aspect ratio for both type 1 and type 2 with Chebyshev distribution of ring-patterned PBG structure.

tribution of the ring PBG units under the transmission line. This is demonstrated in the following results.

Fig. 12(b) shows the measured S-parameters of the uniformly distributed ring-patterned PBG assisted microstrip line. As can be seen, high ripples and low RL are predominant in the passband and a narrow rejection bandwidth is centered at 12 GHz.

2) Nonuniform-Ring PBG Structure With Chebyshev Distribution: We have simulated both type 1 and type 2 nonuniform-ring PBG structures with different aspect ratios. For different aspect ratios, smoother passband before and after low and high cutoff frequencies, respectively, are obtained. For the optimum value of filling factor 0.25, the outer dimensions of the center rings were 56 mil, but we have stretched the limit beyond 1.25 times of the optimum value so that the outer dimensions of the central two elements were 62.5 mil.

The simulated results for the aspect ratio of 0.15 are shown in Fig. 13. Significant improvement in passband ripples at both low and high frequencies is achieved. For different aspect ratios, such as 0.15, 0.35, 0.55, 0.75, and 0.95, all 20-dB rejection bandwidth are calculated. The variation of 20-dB rejection bandwidth with aspect ratio is shown in Fig. 14. As can be seen in this figure, the bandwidth reduces with the aspect ratio. From this figure, it is clear that type 2 is certainly superior to the type 1 PBG structure.

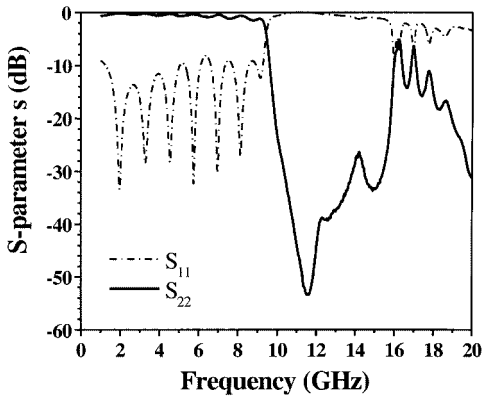

Fig. 15. Measured S-parameters of a 50-Ω transmission line having width $=$ 24 mil on a ring-patterned PBG ground plane. Aspect ratio $= 0.15$ (type 2), $a = 224$ mil, substrate: $\varepsilon_r = 10.2$, $h = 25$ mil.

Finally, prototypes of Chebyshev ring-patterned PBG assisted microstrip transmission lines are fabricated and S-parameters are measured on an HP 8510C vector network analyzer. Fig. 15 shows the measured S-parameters versus frequency plot. A significant improvement of passband ripples and RL and a larger rejection bandwidth of approximately 6 GHz are achieved. This is certainly a significant improvement on ripple height and rejection bandwidth over the conventional PBG assisted transmission lines. Comparing the measured results of Figs. 11 and 15, it can be concluded that the S-parameter performances are far superior in the annular-ring-patterned PBG line.

V. Conclusion

Novel transmission lines in the forms of nonuniform circular-patterned PBG distributions have been studied. Two different distributions—binomial and Chebyshev distributions—applied to low sidelobe array theory have been applied to conventional circular-patterned PBGs and significant improvement over the conventional uniform circular-patterned PBGs have been achieved. While the binomial distributions suffer from narrow bandwidth and lower selectivity, the Chebyshev polynomial distributions improve the performance. It is seen that Chebyshev type 2 distribution has produced similar performance with respect to the rejection bandwidth of conventional uniform distribution of circular-patterned PBGs, but yields significant improvement in selectivity near the cutoff and passband regions.

The nonuniform distributions of circular- and annular-ring-patterned PBGs yield larger bandwidth operation than that for the conventional circular-patterned PBG structure. Both bandwidth and ripple height performances can be improved and controlled with the proper choice of the polynomial distributions of the circular-patterned PBG. It is also seen that the nonuniform distributions of annular-ring-patterned PBG assisted transmission lines have yielded superior performances in all aspects of passband ripples and large stop bandwidth. This technique may be very promising for wide-band planar

antennas, diplexers, filters, amplifiers, and many more high-frequency circuits to come.

REFERENCES

[1] F.-R. Yang, K.-P. Ma, Y. Qian, and T. Itoh, "A uniplanar compact photonic-bandgap (UC-PBG) structure and its applications for microwave circuits," *IEEE Trans. Microwave Theory Tech.*, vol. 47, pp. 1509–1514, Aug. 1999.

[2] M. N. Mollah and N. C. Karmakar, "Planar PBG structures and their applications to antennas," in *IEEE AP-S Int. Symp. Dig.*, Boston, MA, July 2001, pp. 494–497.

[3] R. Coccioli, F. R. Yang, K. P. Ma, and T. Itoh, "Aperture coupled patch antenna on UC-PBG substrate," *IEEE Trans. Microwave Theory Tech.*, vol. 47, pp. 2123–2130, Nov. 1999.

[4] V. Radisic, Y. Qian, R. Coccioli, and T. Itoh, "A novel 2-D photonic band gap structure for microstrip lines," *IEEE Microwave Guided Wave Lett.*, vol. 8, pp. 69–71, Feb. 1998.

[5] S. Collardey, G. Poilasne, A. C. Tarot, P. Pouliguen, C. Terret, and K. Mahdjoubi, "Metallic photonic bandgap propagation mode characterization," *Microwave Opt. Technol. Lett.*, vol. 28, no. 6, pp. 434–440, Mar. 2001.

[6] M. A. G. Laso, T. Lopetegi, M. J. Erro, D. Benito, M. J. Garde, and M. Sorolla, "Novel wideband photonic bandgap microstrip structures," *Microwave Opt. Technol. Lett.*, vol. 24, no. 24, pp. 357–360, Mar. 2000.

[7] T. Lopeteg, M. A. G. Laso, M. J. Erro, D. Benito, M. J. Garde, F. Falcone, and M. Sorolla, "Novel photonic bandgap microstrip structures using network topology," *Microwave Opt. Technol. Lett.*, vol. 25, no. 1, pp. 33–36, Apr. 2000.

[8] M. Qiu and S. He, "High directivity patch antenna with both photonic bandgap substrate and photonic bandgap cover," *Microwave Opt. Technol. Lett.*, vol. 30, no. 1, pp. 41–44, July 2001.

[9] N. C. Karmakar, "Theoretical investigations into binomial distributions of photonic bandgaps on microstripline structures," *Microwave Opt. Technol. Lett.*, vol. 33, no. 3, pp. 191–196, May 2002.

[10] ——, "Improved performance of photonic bandgap microstripline structures using Chebyshev distribution," *Microwave Opt. Technol. Lett.*, vol. 33, no. 1, pp. 1–5, Apr. 2002.

[11] S. Y. Lin and K. L. Wong, "A conical-pattern annular ring microstrip antenna with a photonic bandgap ground plane," *Microwave Opt. Technol. Lett.*, vol. 30, no. 3, pp. 159–161, Aug. 2001.

[12] T. Y. Yun and K. Chang, "Uniplanar one-dimensional photonic-bandgap structures and resonators," *IEEE Trans. Microwave Theory Tech.*, vol. 49, pp. 549–553, Mar. 2001.

[13] C. A. Balanis, *Antenna Theory Analysis and Design*, 2 ed. New York: Wiley, 1997.

[14] R. E. Collin, *Foundations for Microwave Engineering*, 2 ed. New York: McGraw-Hill, 1996.

[15] N. C. Karmakar and M. N. Mollah, "Microstrip lines on annular ring photonic band-gap structures," *Microwave Opt. Technol. Lett.*, vol. 32, no. 6, pp. 431–433, Mar. 2002.

Nemai Chandra Karmakar (S'91–M'91–SM'99) was born in Satkhira, Bangladesh. He received the B.Sc and M.Sc degrees in electrical and electronic engineering from the Bangladesh University of Engineering and Technology, Dhaka, Bangladesh, in 1987 and 1989, respectively, the M.Sc. degree in electrical engineering from the University of Saskatchewan, Saskatoon, SK, Canada, in 1991, and the Ph.D. degree from the University of Queensland, Brisbane, Qld., Australia, in 1999. His doctoral dissertation concerned switched beam and phased-array antennas for mobile satellite communications. His doctoral research was one of the most significant findings at The University of Queensland in 1998 and was published in national media such as *ABC Radio* and the *Canberra Times*.

From 1989 to 1990, he was an Assistant Engineer with the Electronics Institute, Atomic Energy Research Establishment, Dhaka, Bangladesh. In August 1990, he was a Research Assistant with the Communications Research Group, University of Saskatchewan. From 1992 to 1995, he was a Microwave Design Engineer with Mitec Ltd., Brisbane, Australia, where he contributed significantly to the development of land mobile satellite antennas for the Australian Mobilesat. From 1995 to 1996, he taught final-year courses on "Microwaves and Antenna Technologies" at the Queensland University of Technology, Brisbane, Australia. From September 1998 to March 1999, he was a Research Engineer with the Radar Laboratory, Nanyang Technological University, Singapore. Since March 1999, he has been an Assistant Professor and Graduate Advisor with the Division of Communications, School of Electrical and Electronic Engineering, Nanyang Technological University. He has authored or coauthored over 80 referred journal and conference papers, and three book chapters. His research interests concern broad-band microstrip antennas and arrays, smart antennas, beam-forming networks, planar electromagnetic bandgap structures, near-field/far-field antenna measurements, microwave device modeling, and monostatic and bistatic radars. He appeared in the 2002–2003 Marquis *Who's Who in Science and Technology* for his contribution in planar phased arrays.

Mohammad Nurunnabi Mollah was born in Jhenidah, Bangladesh, in 1964. He received the B.Sc. degree in electrical and electronic engineering from the Bangladesh Institute of Technology (BIT), Rajshahi, Bangladesh, in 1986, the M.Sc. degree in electrical and electronic engineering from the Bangladesh University of Engineering and Technology (BUET), Dhaka, Bangladesh, in 1997, and is currently working toward the Ph.D. degree in electrical and electronic engineering from the Nanayang Technological University, Singapore. His doctoral research concerns reconfigurable phased-array antennas using PBG structures.

In 1990, he joined the Department of Electrical and Electronic Engineering, BIT, Khulna, as a Lecturer and became an Associate Professor in 1998. He has authored or coauthored 18 papers in referred journals and conferences. His research interests include microstrip patch antennas and arrays, microwave passive devices, and electromagnetic bandgap structures. Mr. Mollah is a Senior Member of the Institution of Engineers Bangladesh (IEB).